MAT JOURNALS

Journal of Structural and Transportation Studies
Volume 2 Issue 2

On The Non-Linear Finite Element Modelling of Self-Compacting Concrete Beams

Lemuel Thompson Yaw, Jack Banahene Osei and Mark Adom-Asamoah
Department of Civil Engineering,
Kwame Nkrumah University of Science and Technology
jobanahene.coe@knust.edu.gh

Abstract

Self-Compacting Concrete (SCC) is a form of concrete that is able to compact itself under its own weight. Many experimental researchers have resorted to trying to understand the behavioural properties of SCC used in structural elements such as beams. Nonetheless, the validation of the responses of small-scale components using finite element analysis can help engineers to parametrically characterise the behaviour of large-scale components. This study proposes a finite element model to analyse two different SCC beams by using the computational platform, ABAQUS. The load-deflection curves of tested beams was primarily used for verification purposes, with theoretical code-based estimates serving as benchmark. Results indicated that the FEM model compared very well with the experimental responses observed in terms of deformation and load capacities at first crack and ultimate failure. The absolute error in the responses for the developed finite element model was on the average 2.3% and 7.8% for the ultimate failure loads and deflections respectively.

Keywords*: self-compacting concrete, finite element, beam; reinforced concrete*

Correspondence
Jack Osei Banahene, , PMB KNUST, +233-208968363

INTRODUCTION

Concrete has proved to be a very useful construction material of building structures due to its versatility in taking on any structural shape. The introduction of steel as reinforcements into concrete immediately revolutionized the construction industry, new frontiers could be defined and reinforced concrete - as it became known, could be pushed to its structural limits. . In recent years, researchers and practitioners have developed a new type of concrete material called the self-compacting concrete (SCC). This type of concrete is able to flow under its own weight without the need for vibration. This makes it arguably cost-effective and more durable. To better understand the properties of this new kind of concrete, researches set-out to investigate its mechanical properties and structural responses by using different approaches. Ahmad *et al.* (2016) set out to investigate the properties of self-compacting concrete by comparing it with normal concrete. They investigated the compressive and splitting tensile strength of three mixes of concrete NC, SCC and SCC reinforced with fiber glass. The compressive strengths and splitting tensile strengths of SCC were found to be slightly higher than their corresponding NC specimen. Also, the modulus of rapture and modulus of elasticity of SCC were found to be comparatively smaller than NC specimens. This is due to the small quantities of coarse aggregates used in SCC as compared to NC. The increase in compressive strength of SCC is a positive indication of its potential use in construction however, the slightly lower modulus of rapture and elasticity values

could be a downside to its potential. In another study (Akinpelu *et al.* 2017), researchers concluded that the ratio of splitting tensile to compressive strengths for NC and SCC decreases with increasing compressive strengths. The resemblance of SCC to NC in terms of compressive and splitting tensile strengths gives the former an advantageous edge over the later in workmanship terms in the sense that, SCC does not require vibrators and much skilled labour. For this reason, many researchers have continued to investigate the properties of SCC and one particular property that is of much concern is its shear strength in beams. This is because since less coarse aggregates are used it is likely that cracks will propagate in the beams easily. Hassan *et al.* (2008) experimented into the shear strength of SCC beams with no shear reinforcement to better understand the unreinforced behaviour of SCC in shear. Results indicated that the ultimate shear strength of SCC beams is lower than that of NC beams and may be more pronounced in specimens with reduced longitudinal steel reinforcement and with increase in beam depth. A similar conclusion was drawn by Biolzi *et al.* (2014) who performed a four-point bending teste of beams with and without shear reinforcements.

Experimental based testing has been the preferred choice in studying the responses of normal and SCC elements under loading. This method produces real life responses that can be assured of very high accuracies provided the reinforced concrete (RC) elements tested have been developed according to codes of practice and specifications. In so doing, the overall experimental procedure tends to be very expensive and time consuming. Hence a numerical model that allows for verification of the responses of small-scale components is much more preferred option when characterising the behaviour of such reinforced concrete elements. One of the most widely used approaches is the finite element model (FEM). This method has been developed and refined over the years to suit various fields of study. Ever since the introduction of the FEM into civil engineering, many researchers have resorted to studying the behaviour of concrete structures using this new approach. To make FEM a faster and easier method for analysis, computer based software platforms have been developed to help in the complex numerical computations required. With the progression of knowledge and capabilities of computer software and hardware, tremendous improvements in these platforms have been made. This has made FEM modelling on computer platform a preferred choice to most researchers. This method has proved to be far-less expensive and faster. However, in order to ascertain the accuracy of the results from an FEM model, one must fully understand what is being solved in the model and perform the necessary checks to validate the results. These checks could be made by comparing output results from the model with theoretical results or with experimental results.

Farherty (1972) presented one of the earliest works on application of FEM for validating experimental responses for reinforced concrete beams. By modelling the non-linear concrete, assuming a bi-linear idealization of the constitutive behaviour of steel, and with a linear bond-slip material model, predicted structural deformations were similar to those observed in the laboratory. Later Frank Vecchio (1989) proposed a framework for performing the nonlinear finite element modelling based on a smeared crack approach (defining the constitutive behaviour of cracked portion of element section differently). Based on the nonlinear model developed by Frank Vecchio (1989), Barbosa *et al.* (1998) carried out a similar research where a

simply supported reinforced concrete beam subjected to uniformly distributed loading was analysed using ANSYS (a finite element computational platform). After testing the appropriateness of a series of proposed and idealized FEM models of the material behaviour of the beam constituents, it was realized that the best result came from the model which had elastoplastic properties and discrete reinforcement for steel and had multilinear work hardening (Von Mises) for concrete. The predicted ultimate failure loads of this model were very close to those observed in the laboratory. In another study Floros *et al.* (2013) , where the post-cracking bond slip interaction between steel and concrete was considered in a smeared crack FEM model, results were satisfactory in predicting crack width of beams. Badiger *et al.,* (2014) also used finite element to study and analyse beam models by conducting non-linear static analysis. By using ANSYS with a Von-Mises's failure criterion for concrete with multilinear isotropic properties, the results obtained proved that the modelled concrete was capable of predicting the load deflection curve obtained in the laboratory with great accuracy.

One challenge that is affecting the use of SCC as a construction material is the fact that its properties are not well known. Most of the existing research work on the FEM analysis of concrete elements were performed on normal concrete beams. There is therefore a lack of credible data and the need to characterise the behaviour of SCC beams so as to allow the analytical simulation of SCC beams in buildings, bridges etc before construction can begin especially in this era of performance based design for seismic regions. This research paper presents a study on FEM modelling of 2 reinforced SCC beams tested in the laboratory in order to predict the structural behaviour as a means of simulating differently sized SCC beams for design on the ABAQUS FEM platform.

METHODOLOGY

This research is based on the validation of SCC beams that were experimentally in the KNUST structural engineering laboratory. There were two beams in total, all loaded monotonically (see Table 1).

***Table 1**: Table of experimental beams*

Beam label	Dimensions (mm)	Reinforcement ratio (%)	Loading type
LM2-A1	110 x 275 x 2000	1.7	Monotonic
LM2-B1	110 x 275 x 2000	1.3	Monotonic

The various parameters defining the properties of the beams are outlined in Table 2. All beams were loaded at two points through an I-section steel element that received the main load. The loading arm from the supports was 600 mm from each end. The supports were positioned at 100mm distances from each free-end of the beams. This made the effective length of the beams to be 1800mm. Figure 1 below shows how the loading of the beams was carried out.

***Table 2**: Experimental beam properties*

Beam	Compressive Strength F_{cu} (N/mm^2)	Modulus of Rapture F_t(N/mm^2)
LM2-A1	30.2	3.4
LM2-B1	30.2	3.4

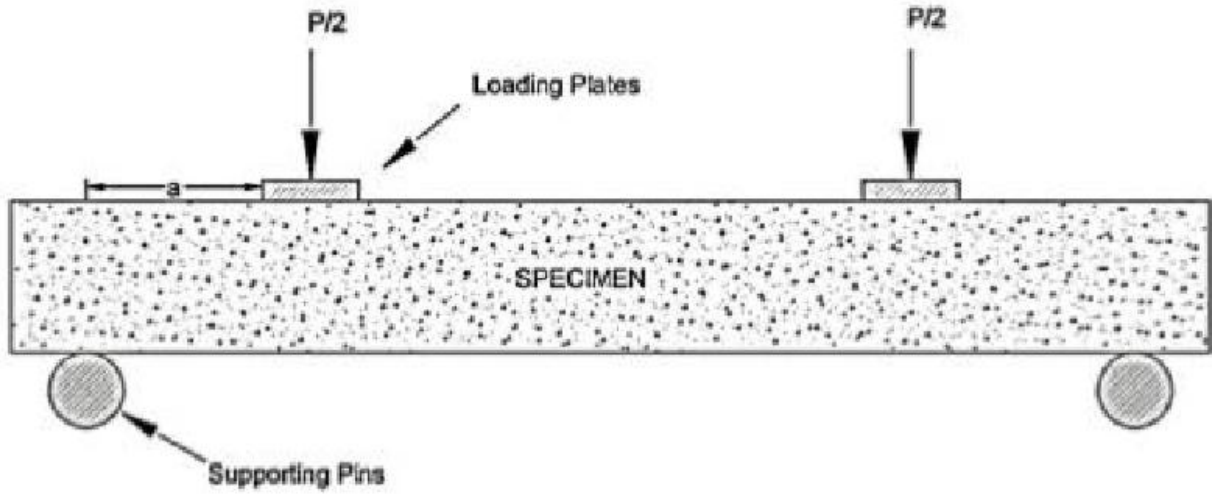

Fig 1: *Schematic experimental setup*

Material Properties

The material properties incorporated into the ABAQUS software (FEM computational platform) is key to defining the responses given by the model in the output. As summarized in the introductory section, a good model is one that can closely follow responses obtained in the lab. In order to do this the material properties specified must correspond to those used in the experimental approach.

Steel as reinforcement

The steel material used to model in ABAQUS was assumed to be linear elastic with a yield strength of 425 MPa and a plastic strain of 0. The elastic modulus of the steel material was set to be 210 GPA and its poison ratio to be 0.3. The elastic modulus and poison ratio altogether form the elastic isotropic properties. These values holistically define the steel material and will be applied to the Beam element in ABAQUS.

Steel as support and loading plates

Steel plates are provided within the model to serve as supports and loading points. The loading plate was necessary to make for easy application of loads as point loads on the required nodes. They have an elastic modulus of 210 GPA and poison ratio of 0.3.

Concrete Properties

Concrete is a very delicate material whose behaviour is different under different situations. This is true for both NC and SCC. Existing literature and relationships between NC and SCC were employed to estimate the properties of SCC. The tensile strength of SCC is within the range 8-15% of its compressive strength. The concrete material has a compressive and tensile strength that varies with the aggregate size used. PCI (2003) states that, the elastic modulus of SCC could be as low as 80% that of NC. It all depended on the paste volume and aggregate type. Equation 1 relates the elastic modulus of NC to its compressive strength.

$$E_c = 4700\sqrt{f_c'} \quad (1)$$

where f_c' is the ultimate strength in N/mm^2 and E_c is the elastic modulus. We took 80% of E_c as the elastic modulus of SCC to account for it being slightly lower than that of NC. The poison ratio was assumed to be 0.2. To guide the non-linear stress strain behaviour of the concrete model, a compressive uniaxial stress-strain curve was incorporated into ABAQUS. The compressive uniaxial stress-strain curve was obtained from the following equations;

$$f = \frac{E_c \varepsilon}{1 + \left(\frac{\varepsilon}{\varepsilon_0}\right)^2} \quad (2)$$

$$\varepsilon_0 = \frac{2 f_c'}{E_c} \quad (3)$$

$$E_c = \frac{f}{\varepsilon} \quad (4)$$

where f = stress at any strain ε (MPa), ε = strain at stress f, ε_0 = strain at the ultimate compressive strength f_c'. This stress-strain curve in Figure 2 was applied to the 3D stress element in ABAQUS as the compressive behaviour under the concrete damage plasticity option. The compressive behaviour stress-strain curve requires the user to input the first point of the curve. It must satisfy Hooke's Law;

$$E = \frac{\sigma}{\varepsilon} \quad (5)$$

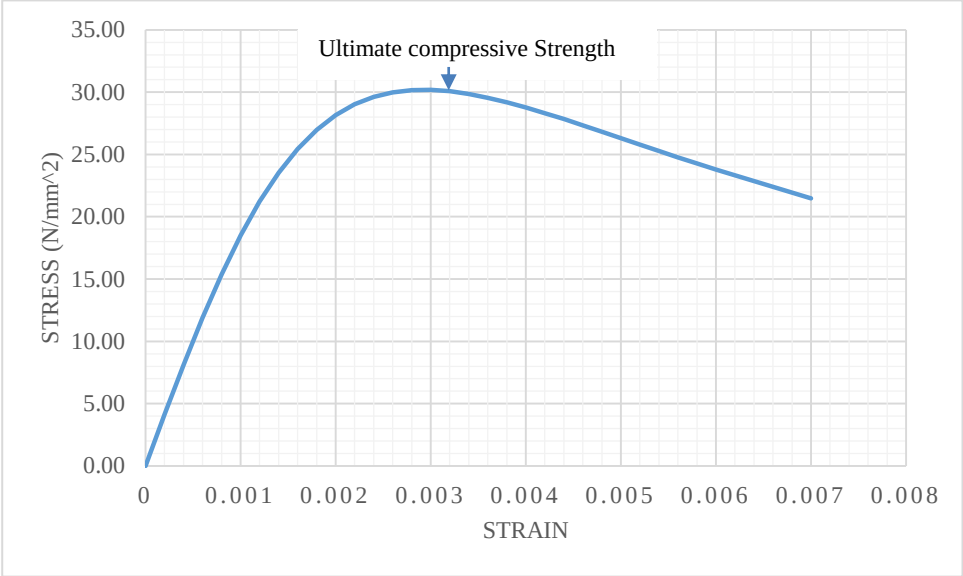

Fig 2: *Uniaxial stress-strain curve for LM2-A1 and LM2-B1*

The ABAQUS software requires the user to input the tensile behaviour of the concrete element. This is important in order to fully capture the post-cracking resistance of concrete to help make more realistic predictions of deflections, bond and shear transfer characteristics of the material. Similar to the compressive stress-strain curve, a curve to guide the tensile behaviour of the concrete element was defined. This curve helps define the cracking strains of the concrete element when cracking begins. It was assumed that cracking of the concrete model began after the ultimate tensile strength was exceeded. Using equation (6) the concrete tensile stress strain curve could be plotted as shown in Figure 3.

$$f_t = 0.306\left(f'\right)^{2/3} \quad (6)$$

where f_t is the tensile stress at any compressive stress f

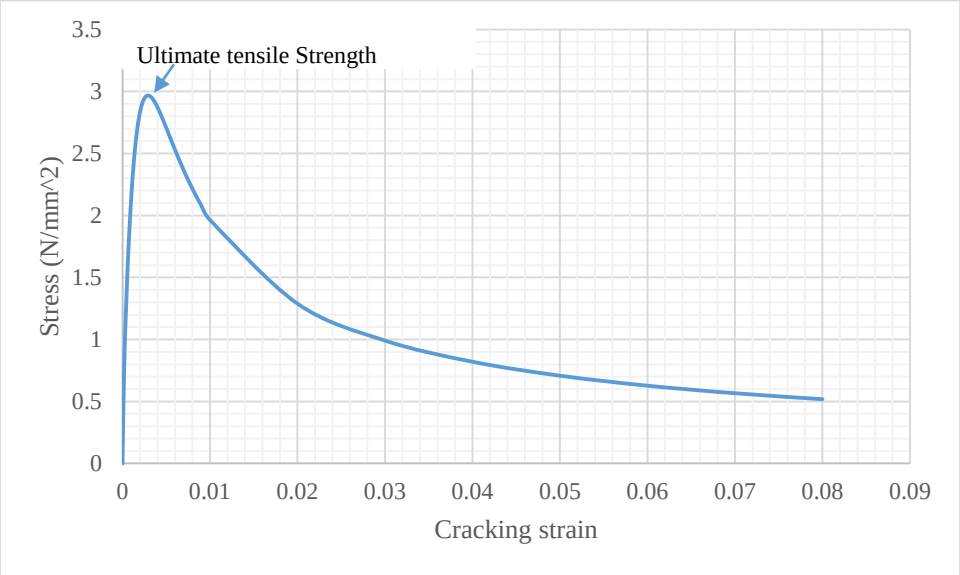

Fig 3: *Uniaxial tensile yield Stress-cracking Strain curve for LM2-A1 and LM2-B1*

Since the stress-strain diagram in Figure 3.3 before the ultimate tensile stress is almost linear with very little changes in strains, the descending portion of the curve after the ultimate tensile strength was also incorporated during the modelling phase.

ABAQUS Finite Element Model

The material properties described above needed to be applied to certain elements within the ABAQUS software. The selected elements must be able to exhibit properties of the material it mimics. Within the ABAQUS material library, there are solid and beam elements that are suitable for modelling. The solid elements are volumetric and the beams require cross-sectional areas specifications. In modelling, two elements were selected based on their suitability; 3D stress element and beam element.

Element type: 3D stress (C3D8R)

To fully model the nonlinear behavior of concrete in ABAQUS, the concrete damage plasticity model (CDP) was used. It works based on the isotropic damage elasticity concept with isotropic tensile and compressive plasticity. This model was applied to the three dimensional stress element (C3D8R) for the concrete properties. The 3D stress element was used to model the concrete material and the steel plates. This element has 8 nodes with reduced integration at one point. To effectively cause this element to simulate damage of concrete in both the tensile and compressive regions, concrete compressive damage parameters (Dc) and concrete tensile damage parameters (Dt) were specified in the model. These parameters help capture to some extent the cracking patterns and crushing patterns in the concrete model. The damage parameters are calculated using the following equation;

$$Dt = 1 - \left(\frac{ts}{ts\,\max} \right) \quad (7)$$

$$Dc = 1 - \left(\frac{Cs}{Cs\,\max} \right) \quad (8)$$

where ts is the tensile stress, ts max is the maximum tensile stress, Cs is the compressive stress and Cs max is the maximum compressive stress.

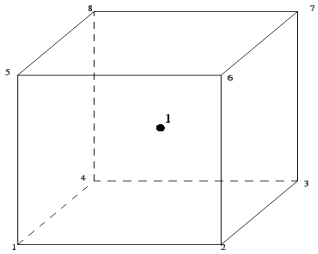

Fig 4: *C3D8R element*

In addition to the damage parameters, the concrete damage plasticity model requires the user to input the plasticity properties related to the concrete model. Some fundamental parameters required to define the concrete damage plasticity model are given in the Table 3.

***Table 3**: CDP parameters for material definition of concrete*

Parameter	Value	Description
β	20	Dilation angle
$\mathcal{E}$	0.1	Eccentricity
Fb_0/fc_0	1.16	Ratio of initial equibiaxial compressive yield stress to initial uniaxial compressive yield stress
K	0.667	Ratio of the second stress invariant on tensile meridian
μ	0	Viscosity parameter

These parameters were applied to the F.E models. With reference to the steel plates, only the elasticity property of the material in Table 4 was specified and applied to the C3D8R element.

***Table 3.4**: Elasticity properties for material definition of steel plate*

EX(Elastic modulus)	Poison ration
210 GPA	**0.3**

Element Types: Beam

A Beam31 element was used to model the reinforcement. This element is a 2-node linear element in 3D with 1st order (linear) interpolation.

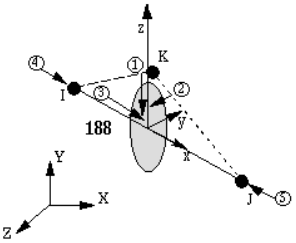

***Fig 5:** Beam31 element*

***Table 5**: Table of Beam31 properties*

EX(Elastic modulus)	210 GPa
Poison ratio	0.3
Yield stress	425 MPa
Plastic strain	0

Modelling

In modelling the beam, the concrete, support plates and loading plates were modelled as volumes (called cells in ABAQUS). The full beam was modelled in ABAQUS. The Table 6 below shows the dimensions of the concrete, support plates and loading plates volume in the respective three orthogonal axes.

***Table 6**: Dimensions for concrete, loading plate and support plate LM2-A1 and LM2-B1*

ABAQUS	Concrete(mm)	Loading Plate1(mm)	Loading Plate2(mm)	Support plate1(mm)	Support plate2(mm)

X-coordinates	0 to 110	0 to 110	0 to 110	0 to 110	0 to 110
Y-coordinates	0 to 275	275 to 300	275 to 300	0 to -25	0 to -25
Z-coordinates	0 to 2000	650 to 750	1250 to 1350	75 to 125	1875 to 1925

The table above specifies the volumetric dimensions of the two support plates, loading plates and full beam. The specified volumes put together are shown in Figure 6 below. The different reinforcement cages were also modelled and their configurations are displayed in the Figure 7 and Figure 8 below. Table 7 gives a breakdown of the reinforcement bars as used in the modelling.

***Table 7**: Reinforcement bar specifications*

Type of reinforcement	LM2-A1 size(mm)	Number	LM2-B1 size(mm)	Number
Top Bar	8	2	8	2
Bottom Bar	12	4	12	2
Shear links	6	20	6	20

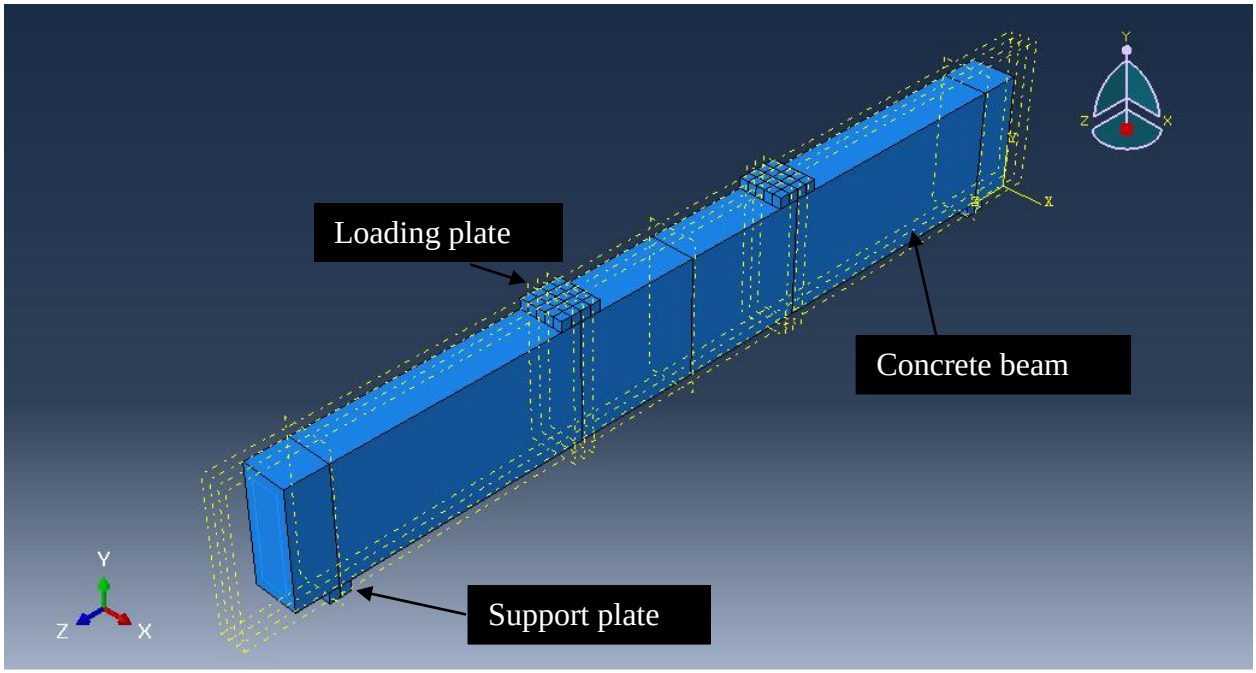

***Fig 6:** Model showing concrete beam, loading plates and support plates for all beams*

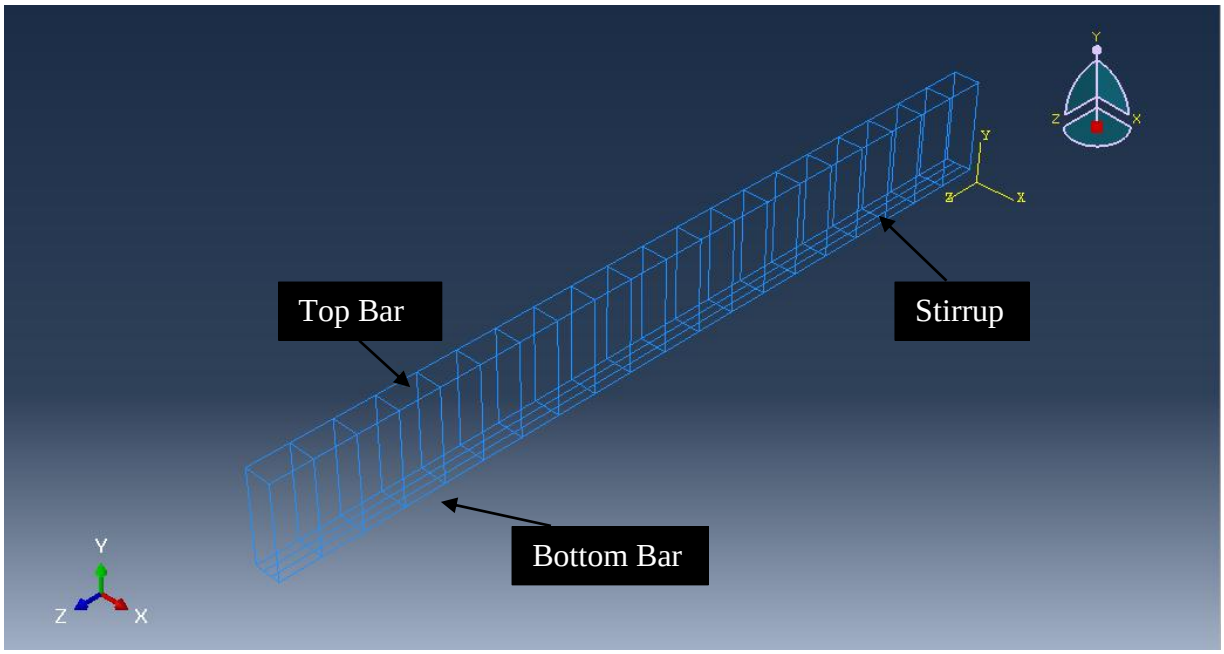

Fig 7: *Model showing rebar cage for LM2-A1*

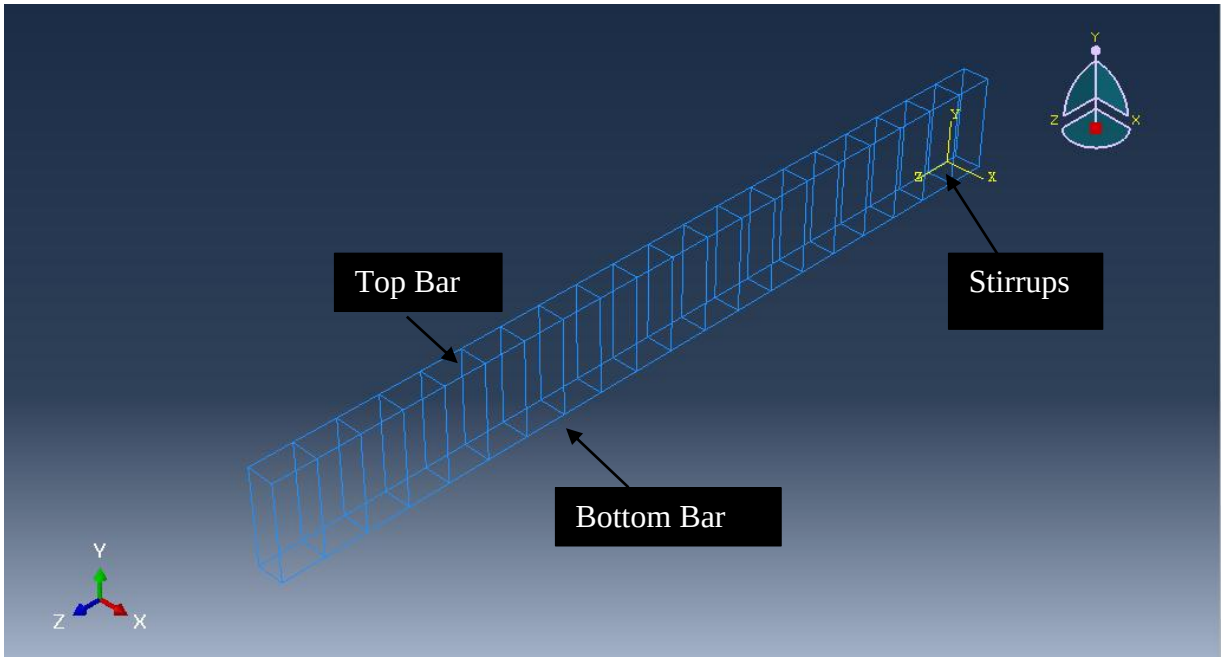

Fig 8: *Model showing rebar cage for LM2-B1*

In order to merge the various reinforcement cages with the concrete volume, ABAQUS has a special constraint feature called "Embedded Region", this was used to constraint the Reinforcement cages to reside within the volume of the concrete. In addition, the reinforcement bars were assigned beam orientations to the default (0,0,-1) within the software. This was necessary to enable the model work properly.

Meshing

In order to achieve good results from the model a rectangular mesh was used. Since all the beams had the same dimensions the same mesh size was used for all. The mesh elements had dimensions of 22 mm x 25

mm x 25 mm. A mesh size of 10 x 10 x 10 mm could have easily been used but this would mean a lot more elements and expensive computational time. During meshing the following mesh attributes were used for each component of the beam.

***Table 8**: Meshing attributes*

Model Parts	Element Type	Material type
Concrete beam	C3D8R	Concrete
Support plate	C3D8R	Steel
Loading plate	C3D8R	Steel
Reinforcement	Beam31	Steel

The overall meshed concrete, loading plates and support plates for all beams is shown in the figure below. It can be noted that the nodes of the steel and loading plates are in alignment with that of the concrete beam. This improves the accuracy of the model and ultimately results that will be obtained. The reinforcement bars were also meshed.

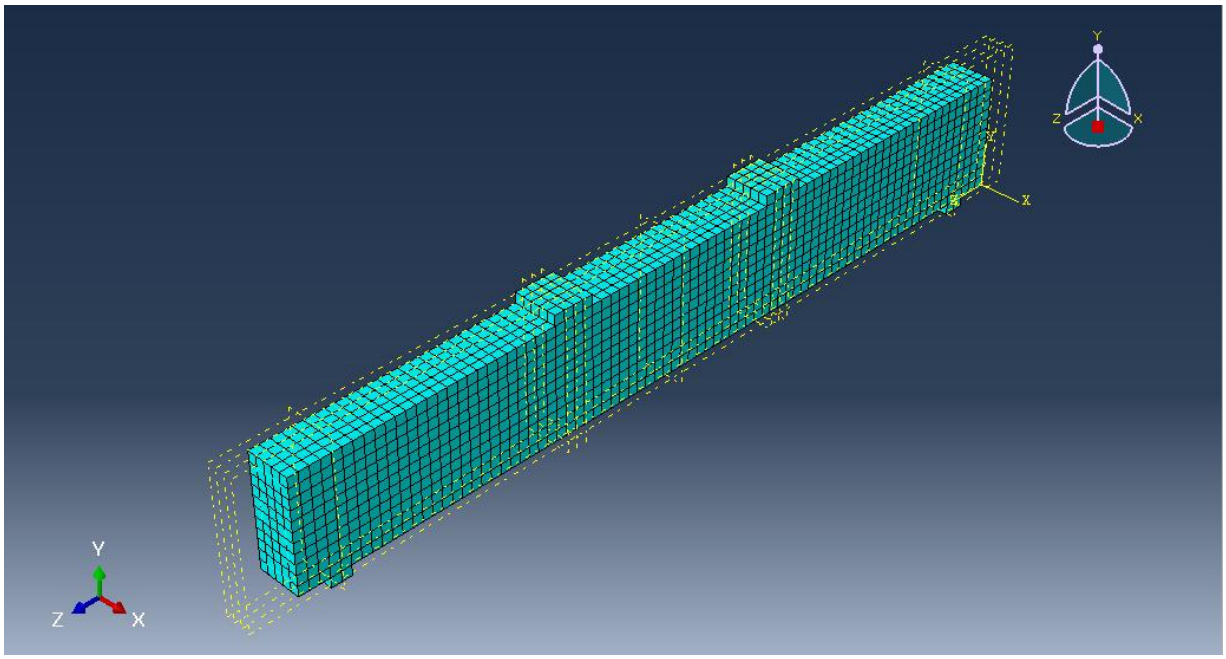

Fig 9: ***Overall meshed model for all beams.***

Loads and Boundary Conditions

To fully imitate the experimental beams, the support conditions have to be modelled in addition. The beams being modelled are simply supported (roller at one end and a pin support at the other). In order to implement these conditions, a line of nodes at the bottom of one of the support was selected and restrained in the U1, U2, U3, UR2 and UR3 as in Figure 10. This allows the support to behave as a pinned support. The beam can then rotate about its transverse axis (x-axis). To better understand the notations above take a look at Table 9.

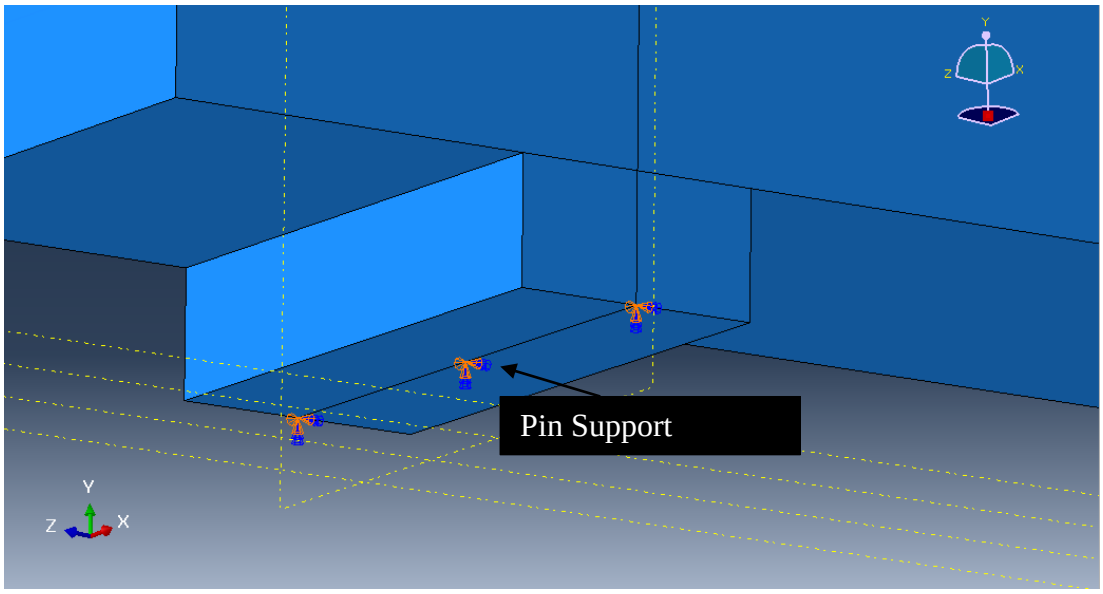

Fig 10: Pinned support restraint condition

***Table 9**: ABAQUS notations and their meanings*

Notation	Meaning
U1	Displacement in the x-axis
U2	Displacement in the y-axis
U3	Displacement in the z- axis
UR1	Rotation about the x- axis
UR2	Rotation about the y-axis
UR3	Rotation about the z- axis

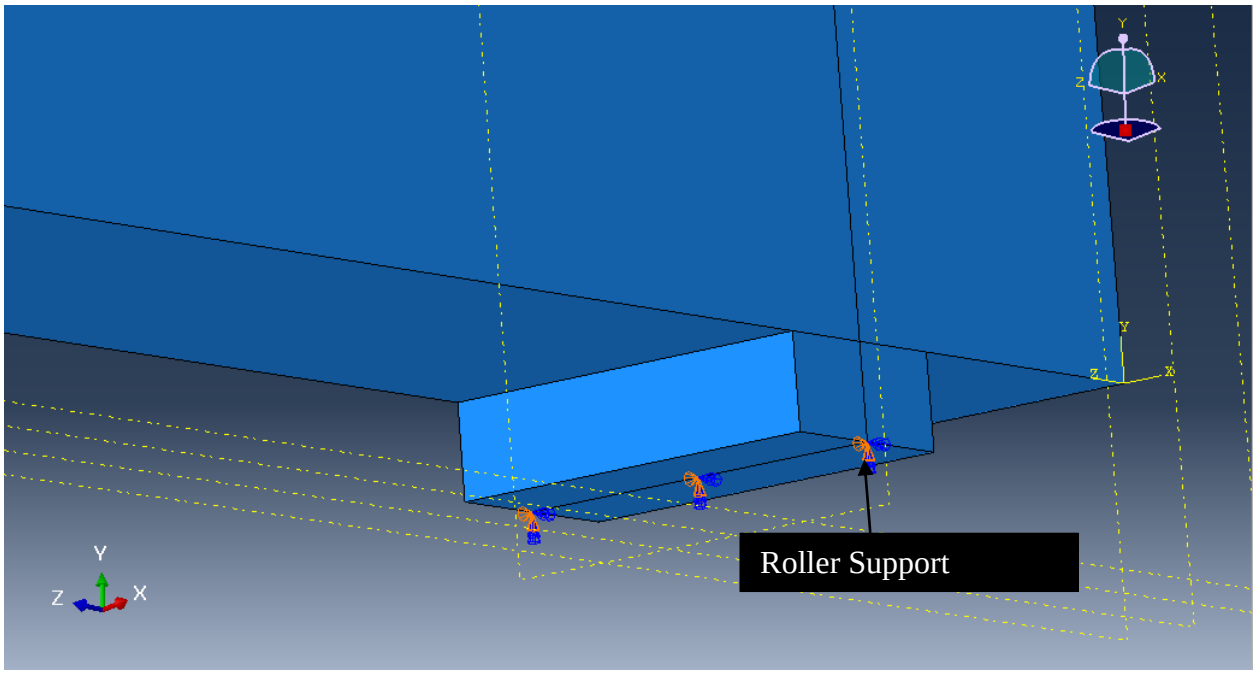

***Fig 11:** Roller support restraint condition*

Similarly, as shown in Figure 11, the roller support conditions were specified. Displacement restrictions were imposed through U1, U2, UR2 and UR3 being set to 0. This allowed the support to rotate

about the x-axis and to displace through the Z- axis.

Half the ultimate loads corresponding to the total failure of the beam specimens in the laboratory was applied on the each of the loading plate located 600mm from the nearest support. The mid-nodes of the plates were selected and the load was applied along them as shown in Figure 12. Each node was made to carry one-sixth of the load on the loading plates. Table 10 below shows the different beam specimens along with their failure experimental loads and their model loads.

***Table 10**: Loading table*

Beam label	Experimental failure load (KN)	Model loads (KN)	ABAQUS load on nodes (KN)
LM2-A1	152	160	13.33
LM2-B1	102	106	8.8333

The monotonic loading was done from zero with load increments in steps of two until the beam failed totally. It is to be noted that the model loads in the Table 10 do not necessarily correspond to the failure loads of the F.E model. These loads are targeted failure loads, that is to say we expect the models to fail before or at these loads. To measure the deflections, the node that corresponds to the bottom mid-point of the beam was selected as set as the point of interest in the model.

Analysis Type and Solution Settings

The type of analysis employed affects the accuracy of the results obtained. From the model, the beam is simply loaded with a static force and we require the displacements, strains, rotations etc. as outputs. This makes the model mechanism a static one since these outputs do not vary with time. The small displacement static option was used since we do not expect our model to undergo very large deflections (see Figure 13). A time increment of 2 was used to increase the load gradually from zero to failure as was done in the experimental approach (see Figure 14). In order to help with convergence of the non-linear solution, a very small minimum step value was specified.

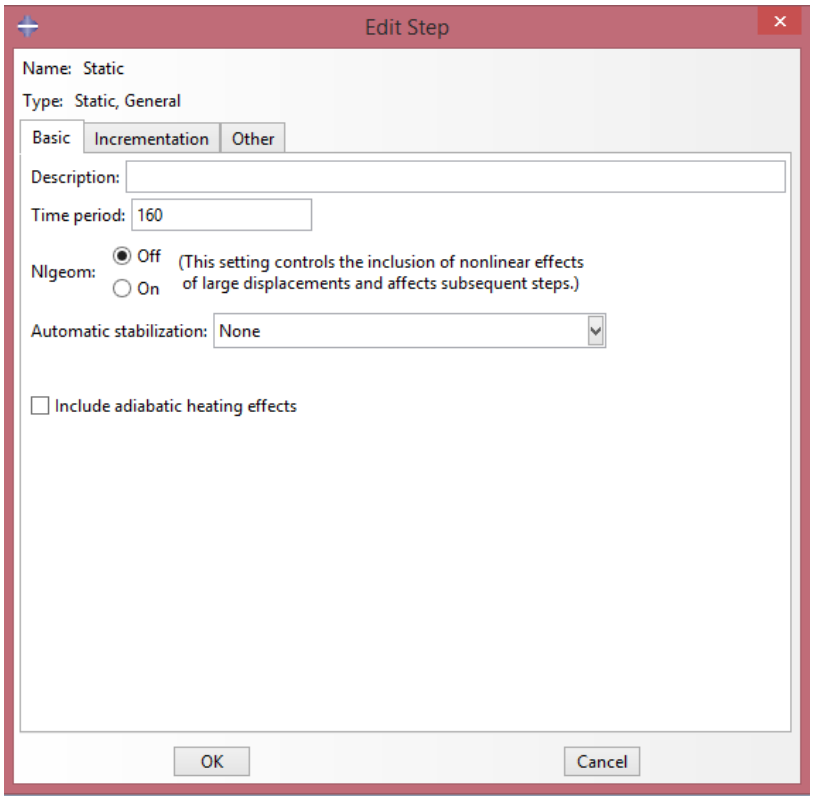

Fig 13: *Sample step controls*

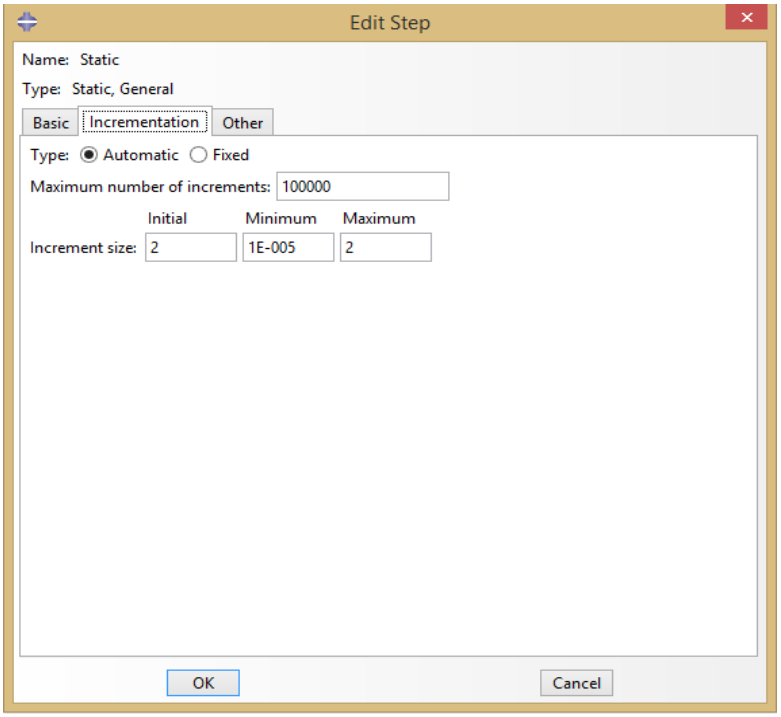

Fig 14: *sample step controls*

Solution Output and Controls

The solution output of the FE model includes the load against mid-span curve and damage distribution in the tension and compression zones. The "history output" requests and "field output" request tabs were used to specify these solution outputs.

RESULTS AND DISCUSSIONS

Behaviour at First Crack Load

During loading of the reinforced SCC beam from 0 KN to load of first crack, the load deflection curve is linear and the beam is in the elastic state. From this curve, the first crack load can be read as the load at which there is a significant change in gradient of the linear line. The initial cracking of the beam occurs when the stress developed in the beam just exceeds rupture modulus of the beam. This occurs in the constant moment region of the beam and is a flexural crack. In order to draw a good comparison between the FE models and the experimental data, both must be compared against a bench mark, in this case theoretical data. The theoretical first crack load required can be computed from elastic equations developed for flexure design of RC beams as shown in the appendix. The theoretical loads, F.E loads and the experimental loads required to cause first crack in the beam have been compared in Table 10 along with their respective deflections.

***Table 10**: Deflection and Load comparisons at first cracking*

	LM2-A1		LM2-B2	
	Load (KN)	Deflection (mm)	Load (KN)	Deflection (mm)
Experimental	34	1.17	24	1.25
F.E	12	0.245	15	0.335
Theoretical	15.7	0.418	16.58	0.430

From the Table 10 above, it can be seen that there is a very good relation between the FE first crack load and the theoretical first crack loads. However, the experimental first crack load seems to be almost twice that of the FE load and the theoretical loads. This can be said to be due to the fact that the crack under-consideration in the theoretical analysis is the first micro-crack to occur. It might not be visible to the naked eye and can be very difficult to find and document in the laboratory. Hence taking this fact into consideration, the crack load for the FE model was then chosen from the full load-deflection curve at the point where there is visible change in gradient of the curve. This gave first visible crack load values as indicated in Table 11.

***Table 11**: Load comparisons at first visible crack*

	LM2-A1	LM2-B1
Experimental load (KN)	34	24
F.E load (KN)	28	20

With this consideration, it can be seen that the load deflection results prior to cracking is good. This implies the FE model is acceptable.

Post-cracking behaviour of SCC Beams

After the linear portion of the beam comes the non-linear response. Within this region the concrete itself can be said to have yielded and is exhibiting inelastic properties. Cracks propagate through the beam as the load is increased. The cracks begin to move out of the constant moment region towards the supports. Diagonal cracks begin to form in the member. ABAQUS is unable to plot crack patterns but is able to plot the damage distribution in both the tension and compression zones in the beam with the help of DAMAGET and DAMAGEC functions. This gives an indication of the cracking patterns in the beam. The Figures 12, 13, 14 and 15

below give illustrations of the damages in the various zones of the FE models.

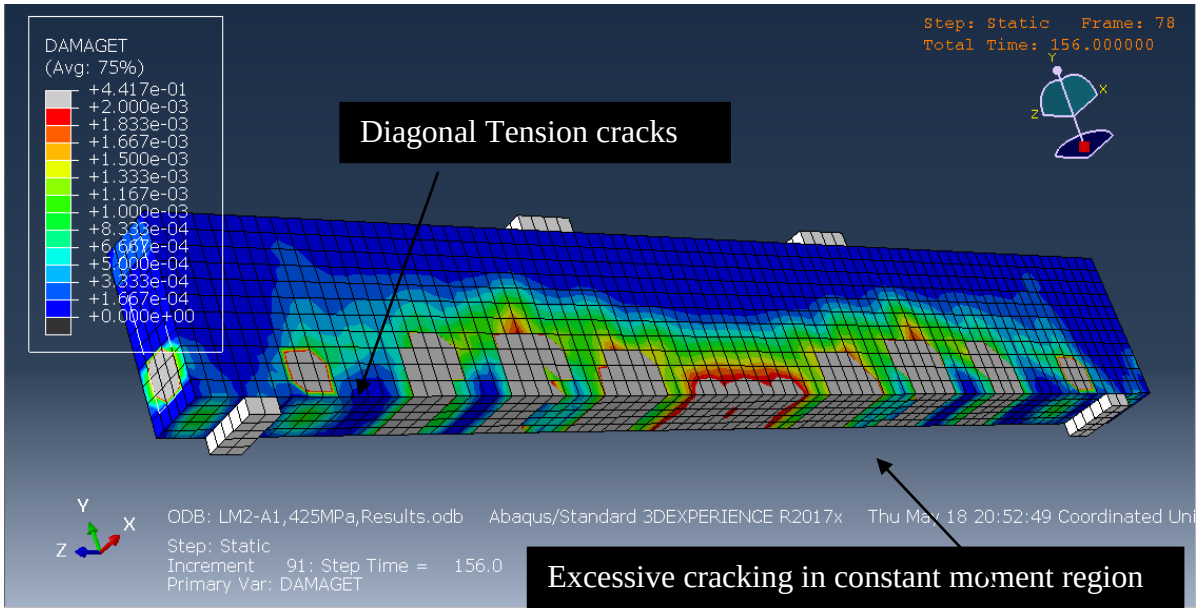

Fig 12: *Tension Damage distribution in LM2-A1 FE model at failure*

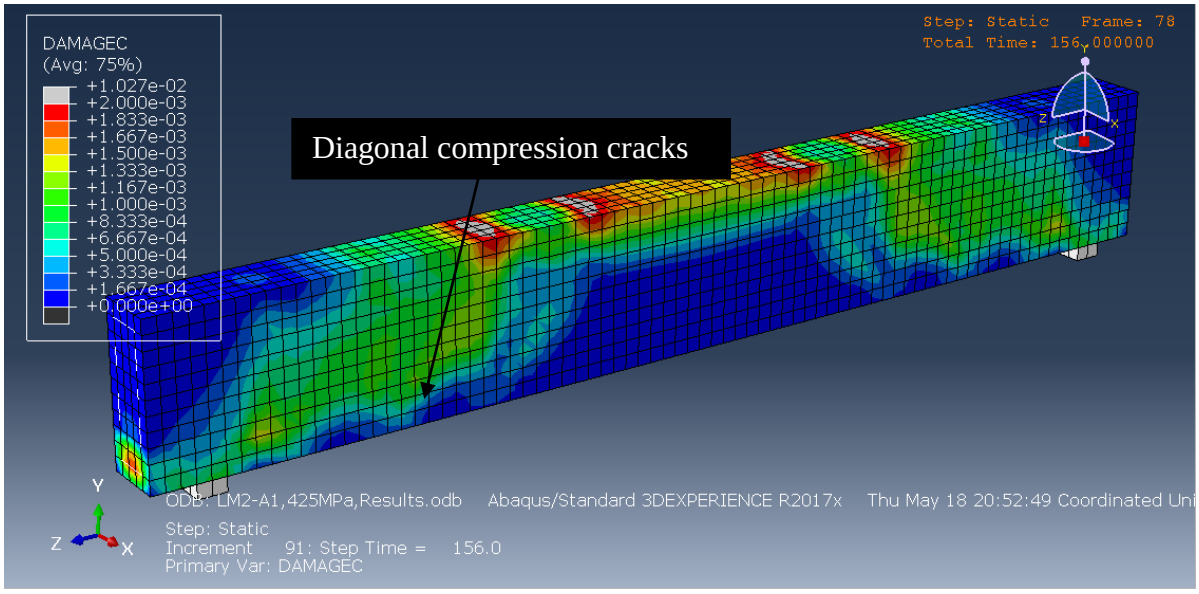

Fig 13: *Compression Damage distribution in LM2-A1 FE model at failure*

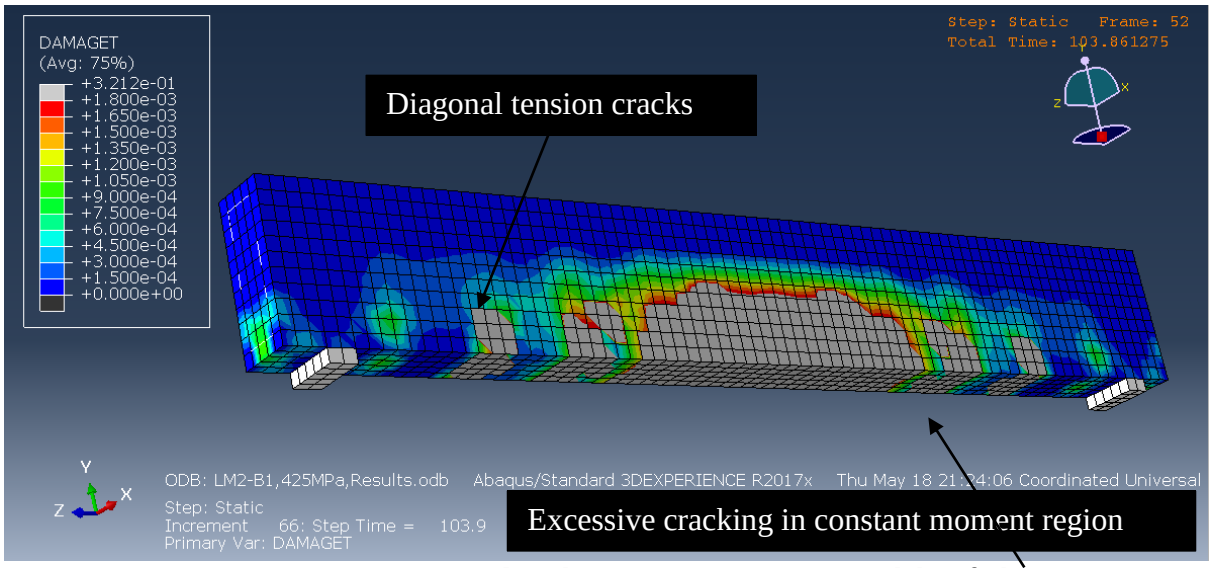

Fig 14: *Tension Damage distribution in LM2-B1 FE model at failure*

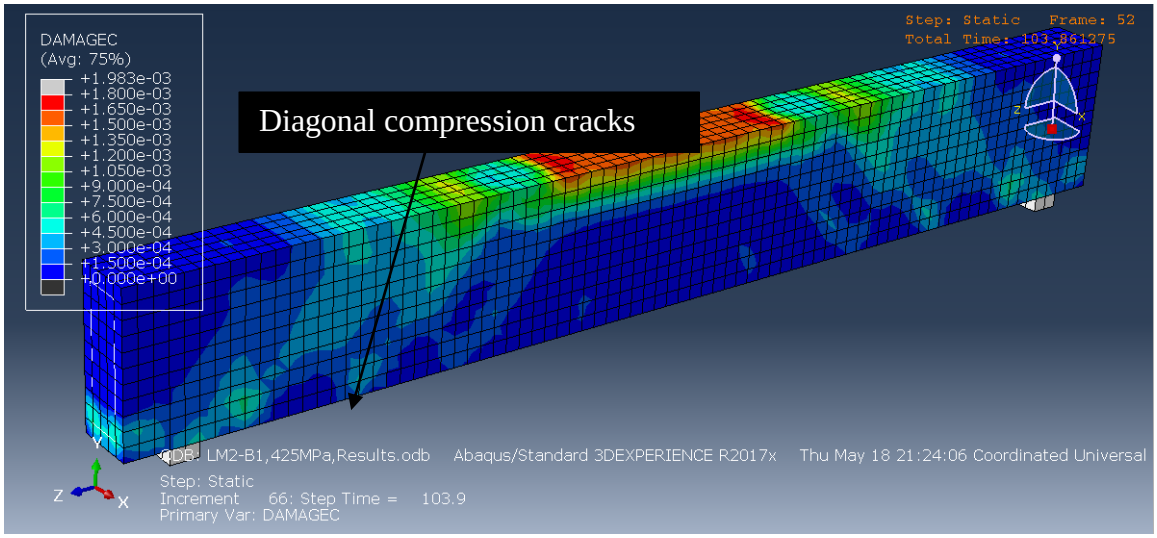

Fig 15: *Compression Damage distribution in LM2-B1 FE model at failure*

Ultimate Failure point

At this load the beam has reached its maximum load carrying capacity and can no longer support any additional load. In the FE model this is indicated by an insurmountable convergence failure of the model whiles in the experimental model a total collapse of the beam specimen. This point is indicated on the various load deflection curves as the last point in the series of plotted points. The maximum deflections of the experimental specimen models and the FE models and their respective failure loads have been compared in Table 12 below.

Table 12*: Failure loads and deflections for LM2-A1 and LM2-B1*

	LM2-A1		LM2-B1	
	Load (KN)	Deflection (mm)	Load (KN)	Deflection(mm)
Exp. Specimen	152	8.6	102	11.2
FE model	156.31	9.4	103.86	10.513

The calibrated finite element models for LM2-A1 and LM2-B1 have shown very good correspondence with their various corresponding experimental specimen data in terms of the deflections and failure loads recorded. The absolute error in the responses for the developed finite element model was on the average 2.3% and 7.8% for the ultimate failure loads and deflections respectively.

Load-*Deflection Response*

The complete non-linear response of the experimental specimens and the FE models have been provided in the Figures 16 and 17 below**.** The responses calculated from the FE model is superimposed on the experimental model's responses. From the graph it can be deduced that there is very good correlation between the FE model and the experimental specimens. This establishes that the material and element models adopted in the FE are satisfactory representations of the experimental beam specimens. This provides confidence in the use of ABAQUS 2017 as a tool for finite element analysis (FEA).

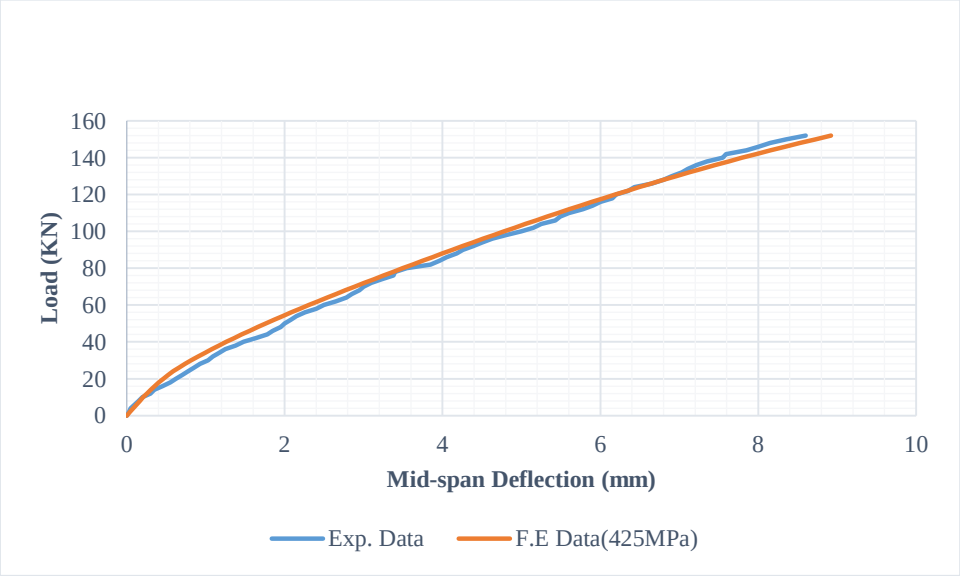

Fig 16: *Graph of Load against Mid-span deflection for Beam model LM2-A1*

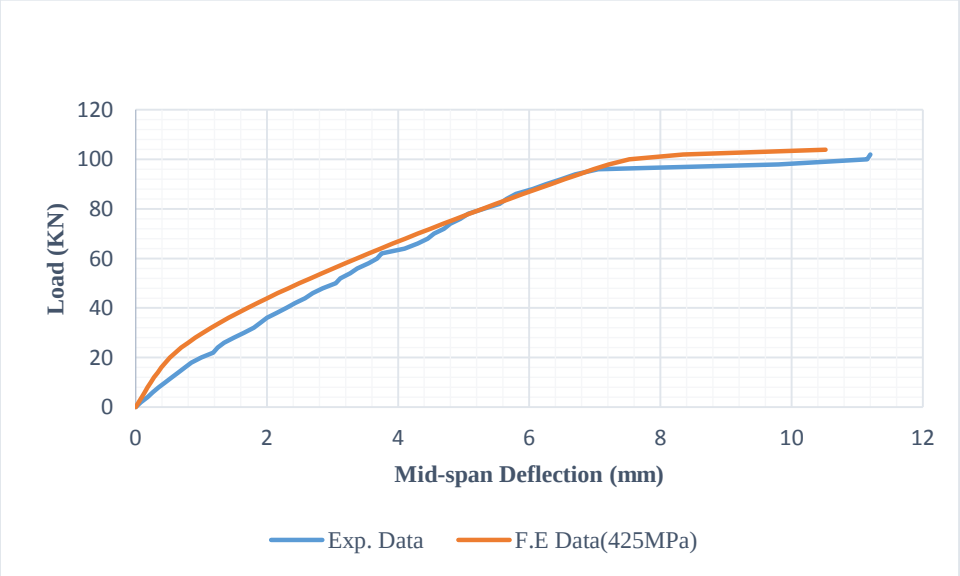

Fig 17: *Graph of Load against Deflection for Beam model LM2-B1*

CONCLUSIONS

In this paper, the FEM was used to analyse SCC beams in order to calibrate and come up with a model that is capable of predicting the responses of SCC beams without the need for experimental methods in order to save time and cut-down on cost. Two reinforced SCC beams were modelled and calibrated to experimental data by analysing them using ABAQUS finite element software. Responses in the form of load-deflection curves and cracking pattern and behaviour were compared to experimental results.

The following conclusions can be drawn from the evaluation of the results obtained from the calibrated models; (1) the mid-span deflections compares well with the experimental data at hand; (2) the failure loads predicted by the calibrated FE models are very close to those observed in their respective experimental models; (3) the loads applied in the FE models to cause initial micro cracking of beam match well with hand calculations; (4) the absolute error in the responses for the developed finite element model was on the average 2.3% and 7.8% for the ultimate failure loads and deflections respectively.

REFERENCES

1. Akinpelu, M.A,Odeyemi, S.O.,Olafusi,O.S & Muhammed,F.Z., 2017. *Evaluation of splitting tensile and compressive strength relationship of self-compacting concrete.* Journal of King Saud University – Engineering Sciences (article in press).
2. Ahmed, S., Umer, A. & Masood, A., 2016. *Properties of Normal, Self Compacting Concrete And Glass Fibre-Reinforced Self-Compacting Concrete: An Experimental Study.* 11th International Symposium on Plasticity and Impact Mechanics, pp. 807-813.
3. Badiger, N.S. & Malipatil, K.M., 2016. *Parametric Study on Reinforced Concrete Beam using ANSYS.* Civil and Environmental Research, pp. 88-94.
4. Biolzi, L., Cattaneo, S. & Mola, F., 2014. *Bending-Shear Response of Self-Consolidating And High Performance Reinforced Concrete Beams.* Engineering Structures, pp. 399-410.
5. Farherty, K., 1972. *An Analysis Of A Reinforced And A Prestressed Concrete Beam By Finite Element Method*, Iowa : Doctorate's Thesis, University of Iowa.
6. Frank, V. J., 1989. *Nonlinear Finite Element Analysis Of Concrete Members*. ACI Structural Journal, pp. 26-35.
7. Barbosa, A. F. & Ribeiro, G. O., 1998. *Analysis Of Reinforced Concrete Structures Using Ansys Nonlinear Concrete Model*. Computational Mechanics: New Trends and Applications, pp. 1-7.
8. Floros, D. & Ingason, O. A., 2013. *Modelling And Simulation Of Reinforced Concrete Beams; Coupled Analysis of Imperfectly Bonded Reinforcement in Fracturing Concrete,* Master's thesis in Solid and Structural Mechanics.. Goteborg, Sweden.
9. Hossain, K. A., Lachemi, M. & Hassan, A., 2008. Behaviour Of Full-Scale Self-Consolidating Concrete Beams In Shear. *Cement and Concrete Composites,* Volume 30, pp. 588-596.